



Peer review status:

This is a non-peer-reviewed preprint submitted to EarthArXiv.

1 Highlights

2 **Rising Temperatures Increase Risk of Soil Salinity and Land**  
3 **Degradation in Water-Scarce Regions**

4 Isaac Kramer, Nadav Peleg, Yair Mau

- 5 • We develop a modeling framework for salinity and sodicity under  
6 changing climate combining SOTE and AWE-GEN models
- 7 • We analyze sensitivity of salinity and soil degradation to changes in  
8 ET and rainfall (season length and extremity)
- 9 • Results show that aridity drives elevated salinity. Increases in salinity  
10 are most sensitive to rising ET.
- 11 • Increased ET leads to greater risk of soil degradation as indicated by  
12 declining saturated hydraulic conductivity

13 Rising Temperatures Increase Risk of Soil Salinity and  
14 Land Degradation in Water-Scarce Regions

15 Isaac Kramer<sup>a</sup>, Nadav Peleg<sup>b,c</sup>, Yair Mau<sup>a</sup>

<sup>a</sup>*Institute of Environmental Sciences, The Robert H. Smith Faculty of Agriculture, Food and Environment, The Hebrew University of Jerusalem, Rehovot, Israel*

<sup>b</sup>*Institute of Earth Surface Dynamics, University of Lausanne, Lausanne, Switzerland*

<sup>c</sup>*Expertise Center for Climate Extremes, University of Lausanne, Lausanne, Switzerland*

---

16 **Abstract**

Climate change introduces significant uncertainty when assessing the risk of soil salinity in water-scarce regions. We combine a soil-water-salinity-sodicity model (SOTE) and a weather generator model (AWE-GEN) to develop a framework for studying salinity and sodicity dynamics under changing climate definitions. Using California's San Joaquin Valley as a case study, we perform first-order sensitivity analyses for the effect of changing ET (a proxy for changing temperature), length of the rain season, and magnitude of extreme rainfall events. Higher aridity, through increased ET, shorter rainy seasons, or decreased magnitude of extreme rainfall events, drives higher salinity – with rising ET leading to the highest salinity levels. Increased ET leads to lower levels of soil hydraulic conductivity, while the opposite effect is observed when the rainfall season length is shortened and extreme rainfall events become less intense. Higher ET leads to greater unpredictability in the soil response, with the overall risk of high salinity and soil degradation increasing with ET. While the exact nature of future climate changes remains unknown,

the results show a serious increase in salinity hazard for climate changes within the expected range of possibilities. The presented results are relevant for many other salt-affected regions, especially those characterized by intermittent wet-dry seasons. While the San Joaquin Valley is in a comparatively strong position to adapt to heightened salinity, other regions may struggle to maintain high food production levels under hotter and drier conditions.

17 *Keywords:* irrigation, salt-affected, climate change, sodicity, hazard,  
18 agriculture

---

## 19 **1. Introduction**

20 Soil salinity and sodicity present major challenges to agricultural  
21 production (Howitt et al., 2009; Wallender and Tanji, 2011; Qadir et al.,  
22 2014; FAO and ITPS, 2015; Daliakopoulos et al., 2016; Práválie et al., 2021;  
23 Kramer and Mau, 2023). High soil salinity inhibits plant water uptake,  
24 leading to declining yields and plant death (McGeorge, 1954; Bernstein,  
25 1975; Maas and Grattan, 1999; Munns, 2002). High sodicity levels can  
26 trigger the breakdown of soil aggregates, limiting the flow of water and air  
27 to the root zone, thereby threatening plant growth (McGeorge, 1954;  
28 Mandal et al., 2008; Levy, 2011; Bardhan et al., 2016). Critically,  
29 experimental and field evidence has indicated that breakdowns in soil  
30 aggregates are extremely difficult to reverse, in many cases causing  
31 permanent soil degradation (Bhardwaj et al., 2008; Assouline and Narkis,  
32 2011; Schacht and Marschner, 2015; Adeyemo et al., 2022).

33 The threats of salinity and sodicity are especially pronounced in

34 water-scarce regions (FAO, 2023). Due to limited freshwater supplies, food  
35 production in these areas often depends on irrigation with high salinity  
36 water, including treated wastewater and saline groundwater (Oster, 1994;  
37 Bixio et al., 2006; Levy, 2011; Assouline et al., 2015). With domestic water  
38 needs typically prioritized over the agricultural sector's, reliance on high  
39 salinity irrigation water is expected to increase over the coming decades  
40 (Oster, 1994; Bixio et al., 2006; Levy, 2011; Assouline et al., 2015; Kramer  
41 et al., 2022b).

42 Climate change introduces an additional element of uncertainty when  
43 forecasting the risk of salinity-induced damage to agriculture. Rising  
44 temperatures and changes to annual rainfall have the potential to further  
45 aggravate water scarcity, pushing growers to even greater dependence on  
46 high salinity irrigation supplies – at a time when plants are already facing  
47 more intense heat stress and atmospheric demand. In areas with distinct  
48 dry and wet seasons, rainfall is often critical in the natural leaching of salts  
49 that accumulate from irrigation (Lado et al., 2012). Changes in rainfall  
50 patterns (e.g., shorter rainfall season, reduction in rainfall amounts, or  
51 increase in intermittency between storms) could disrupt these processes,  
52 leading to a potential rise in average soil salinity levels, and putting the soil  
53 at risk of long-term, irreversible degradation.

54 We seek to understand how the dynamics of salinity and sodicity in  
55 water-scarce regions are most likely to be affected by changing rainfall and  
56 temperature patterns. While the impact of salinity and sodicity on plants  
57 and soils has been closely studied (Minhas et al., 2020; Kramer and Mau,  
58 2023), the effects of climate change on salinity and sodicity have received

59 limited attention. Most research on the intersection of agriculture and  
60 salinity has focused on preventing salinity-driven damage to groundwater  
61 and other natural water resources (Knapp, 1992a,b,c; Dinar et al., 1993;  
62 Hansen et al., 2018; Quinn, 2020). Hassani et al. (2020, 2021) use  
63 data-driven models to try and predict how primary soil salinity (i.e.,  
64 salinity caused by natural processes) will change over the 21st century.  
65 Their models, however, do not apply to secondary salinity (salinity driven  
66 by human activities), such as the irrigation-driven salinity and sodicity that  
67 is common in agricultural-producing regions. Kramer and Mau (2020)  
68 demonstrated that shorter rainy seasons and an increase in the magnitude  
69 of extreme precipitation events have the potential to exacerbate the risk of  
70 salinity- and sodicity-driven soil degradation in agricultural settings. While  
71 the framework used by (Kramer and Mau, 2020) explores only one specific  
72 change in rainfall patterns, without considering feedback loops between  
73 salinity levels and the ability of water to move through the soil, the findings  
74 underscore the fact that climate change may introduce new conditions that  
75 challenge traditional salinity management strategies. Corwin (2021)  
76 evaluate existing research on the impact that climate change has had up to  
77 now. This important review notes that remote sensing is a powerful tool for  
78 monitoring salinity development and emphasises the risk that climate  
79 change is already presenting in important agricultural regions. It is not,  
80 however, a tool for forecasting the effect of specific climate changes on  
81 salinity and sodicity dynamics. In the face of such changes, growers who  
82 don't adapt may be confronted with declining yields and an increased risk  
83 of irreversible soil degradation. Given this possibility, we must develop a

84 core understanding of how anticipated changes in climate may affect  
85 salinity and sodicity trends so that policymakers and extension specialists  
86 can adequately prepare growers to face new challenges.

### 87 *1.1. Case study: the San Joaquin Valley*

88 As a case study for the effects of climate change on salinity and sodicity,  
89 we focus on California’s San Joaquin Valley (SJV). In addition to being one  
90 of the most important agricultural areas in the United States, the SJV is an  
91 apt case study because severely limited freshwater allocations make farmers  
92 dependent on often-saline groundwater supplies for irrigation.  
93 Salinity-driven environmental damage has been a concern and focus of  
94 research in the SJV for more than a century (Nelson et al., 1918; Eaton,  
95 1935; Tanji et al., 1972; Amundson and Smith, 1988; Fujii et al., 1988;  
96 Tidball et al., 1989; Lin et al., 2000; Hanson and May, 2003; Mitchell et al.,  
97 2017; Hansen et al., 2018; Corwin, 2021). The focus of these studies has  
98 ranged from remediation of salt-affected lands (Amundson and Lund,  
99 1985), surveying the extent of existing salinity damage (Scudiero et al.,  
100 2014; Thellier et al., 1990), the hydrological roots of saline groundwater  
101 (Schoups et al., 2005), and mapping root zone salinity using remote sensing  
102 in response to climate changes (Corwin, 2021). We are unaware of any  
103 studies, however, that have considered the role of future climate conditions  
104 on salinity and sodicity dynamics.

105 The present SJV climate is characterized as warm-summer  
106 Mediterranean (Csb) by the Köppen-Geiger classification (Peel et al.,  
107 2007), with a rainy winter season from November to April that yields an  
108 average annual precipitation of 275 mm. Summers in the SJV are warm

109 and dry with virtually no rainfall and a mean daily temperature of 24.6 °C.  
110 This contrast between a wet winter season and a dry summer season is  
111 typical of many salt-affected regions.

112 While climate models project with a high level of certainty that  
113 temperatures in the SJV will rise over the remainder of the 21st century,  
114 they are unclear about the precise magnitude (Pierce et al., 2013).  
115 Projected changes in precipitation patterns are marked by much higher  
116 levels of uncertainty, partly because inter-annual variability in rainfall  
117 amounts in the region is already high (Pierce et al., 2013). Among the most  
118 common probable climate projections are (i) a decrease in the overall length  
119 of the winter rainfall season and (ii) intensification of extreme rainfall  
120 events. The latter is primarily driven by temperature increases (Peleg  
121 et al., 2020; Marra et al., 2024), and therefore is highly probable (Fowler  
122 et al., 2021) even if precipitation levels remain unchanged.

123 We examine how incremental changes in each of these variables –  
124 temperature, rainfall season length, and the magnitude of extreme rainfall  
125 events – are likely to impact the hazard of salinity-induced crop damage  
126 and sodicity-induced soil degradation in irrigated lands. While our focus on  
127 the SJV reflects its central role in US food production, we would like to  
128 point out that many other important agricultural regions across the US  
129 Southwest and Midwest, along with other agricultural regions worldwide,  
130 share similar climate profiles and are susceptible to similar pressures as a  
131 result of water scarcity (Corwin, 2021).



## 132 **2. Material and methods**

### 133 *2.1. Modeling salinity, sodicity, and hydraulic conductivity dynamics*

134 Changes in soil salinity and sodicity, and how they affect saturated  
135 hydraulic conductivity, are modeled using the Salt of the Earth 2.0 (SOTE)  
136 model (Kramer et al., 2022a). SOTE focuses on how irrigation (chemical  
137 composition and application rates) and climate conditions (precipitation  
138 and evapotranspiration fluxes) drive the dynamics of relative soil water  
139 content, the electrolyte concentration of the soil water (i.e., salinity), and  
140 the fraction of sodium ions in the soil’s exchange complex (i.e., sodicity).  
141 As the dynamics of these three state variables evolve, SOTE includes  
142 feedback with saturated hydraulic conductivity,  $K_s$ . In contrast to other  
143 models that track salinity and sodicity dynamics (Šimůnek and Suarez,  
144 1994; Šimůnek et al., 2013; Kroes et al., 2017; Ma et al., 2012; Russo, 1984,  
145 1988; Russo et al., 2004; Russo, 2013; van der Zee et al., 2010; Shah et al.,  
146 2011; van der Zee et al., 2014; Kramer and Mau, 2023), SOTE includes the  
147 potential for irreversible effects when modeling increases and decreases in  
148 soil  $K_s$ . This is important because experimental and field evidence has  
149 demonstrated that changes in  $K_s$  are marked by hysteresis (Bhardwaj  
150 et al., 2008; Assouline and Narkis, 2011; Schacht and Marschner, 2015;  
151 Adeyemo et al., 2022). The exclusion of hysteresis in  $K_s$  has been  
152 demonstrated to significantly lower the forecasted probability of long-term  
153 soil degradation, making its inclusion critical for understanding the actual  
154 risks to soil health (Kramer and Mau, 2020; Kramer et al., 2022a).  
155 Therefore, declines in saturated hydraulic conductivity are often used as a  
156 metric for soil degradation. SOTE can be used to investigate the effect of

157 climate change on salinity and sodicity dynamics by modifying rainfall and  
158 actual evapotranspiration of the crop under non-standard conditions  
159 ( $ET_{c \text{ act}}$ ,  $\text{mm d}^{-1}$ ) (Fernández, 2023). In this setup,  $ET_{c \text{ act}}$  is a proxy for  
160 the effects of temperature. All references to ET in the remainder of this  
161 article refer to  $ET_{c \text{ act}}$ .

162 The salinity, sodicity, and water dynamics in the SOTE model were  
163 successfully validated against results from a multiyear lysimeter experiment  
164 involving different irrigation water qualities and precipitation (Gonçalves  
165 et al., 2006). The hydraulic conductivity module used in SOTE has been  
166 validated through laboratory experiments (Adeyemo et al., 2022; Kramer  
167 et al., 2021). The SOTE model has also been used to examine plant  
168 responses to salinity and sodicity (Yin et al., 2021, 2023).

## 169 *2.2. Generating stochastic weather*

170 The present and future rainfall and evapotranspiration time series were  
171 generated using the 1-dimension version of the AWE-GEN (Advanced  
172 Weather Generator) model (Fatichi et al., 2011; Ivanov et al., 2007). This  
173 hourly weather generator is capable of reproducing the key climatic  
174 variables required for agro-hydrological applications, such as precipitation,  
175 cloud cover, temperature, radiation, and humidity, while preserving their  
176 temporal correlations. The low- and high-order statistics of the generated  
177 time series are realistically emulated by employing physically-based and  
178 stochastic approaches. For example, the precipitation module is based on a  
179 Poisson-cluster process, while the near-surface air temperature module  
180 includes a stochastic component to generate the hourly time series  
181 according to the diurnal cycle and seasonality, physically constrained with

182 the hourly cloud cover and radiation budget. Readers are referred to  
183 (Fatichi et al., 2011) for more information regarding AWE-GEN; Fatichi  
184 et al. (2013) provides an overview of model parameterization for future  
185 climate conditions. AWE-GEN is a robust model that has been used to  
186 generate long and non-stationary time series of climatic variables for  
187 multiple applications (e.g., (Fatichi et al., 2021; Cache et al., 2023; Ramirez  
188 et al., 2023)).

189 The model was calibrated to generate ET and rainfall hourly time series  
190 using 40 years of ERA5 climate data (1980 to 2020) for Fresno County in the  
191 SJV. The model was validated against measured values over the same period  
192 (Supplemental Materials 1). To account for the natural climate variability  
193 (inter- and intra-annual variations), we generated 500 unique years of baseline  
194 rainfall and ET data (Fig. 1).

### 195 *2.3. Simulations framework*

196 The objective of our study is to understand how long-term trends in  
197 salinity and sodicity dynamics will be affected by potential changes in  
198 climate. To facilitate this goal, we use the one-at-a-time technique where  
199 the effect of one parameter (evapotranspiration, rainfall season length,  
200 rainfall intensity) is analyzed while keeping the others fixed. In this local  
201 sensitivity analysis approach (Razavi and Gupta, 2015), variations in  
202 output are then a measure of how susceptible the system is to changes in  
203 that particular input variable. Such a framework enables the  
204 straightforward identification of potential trends, e.g., the effect of  
205 increasing ET on overall salinity or saturated hydraulic conductivity levels,  
206 while avoiding the intense computational demands of a global sensitivity

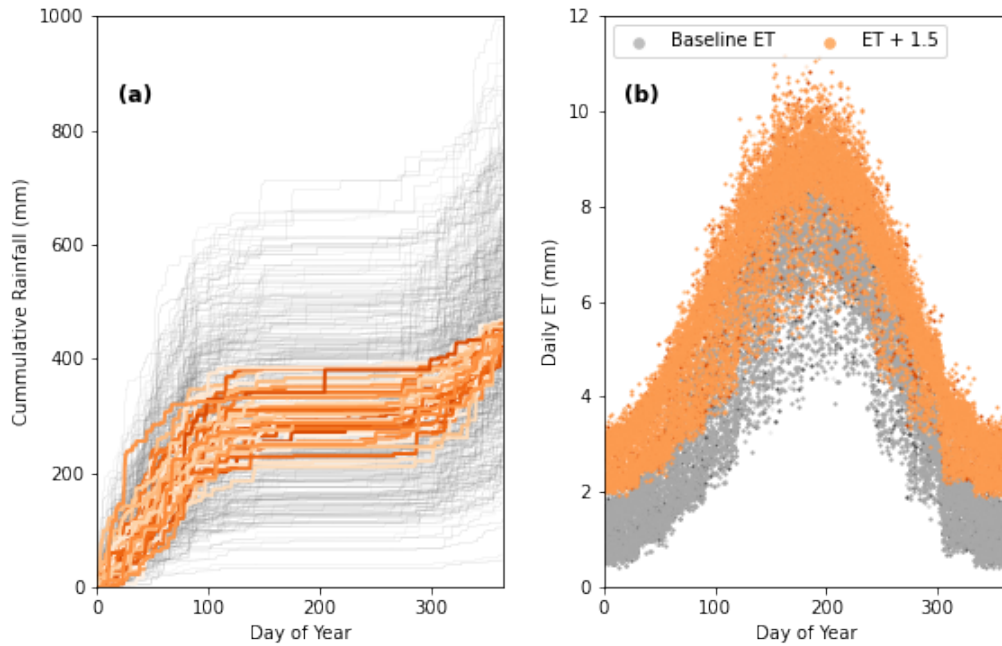


Figure 1: The 500 years of stochastic simulations of rainfall (a; grey lines) and ET (b; grey points) generated using the AWE-GEN model. Orange lines highlight the 50 years in which total annual rainfall was between the 45th and 55th percentiles of the ensemble. Orange points are elevated ET by  $1.5 \text{ mm d}^{-1}$ .

207 analysis. It also allows us to probe for the existence of “cutoff thresholds” –  
 208 points beyond which irreversible soil degradation might occur.

209 To account for natural variations in climate, the simulations are divided  
 210 into scenarios, each composed of a unique set of input conditions. Each  
 211 scenario is made up of a stochastic ensemble of 50 climatic realizations, each  
 212 realization 15 years long, sampled from the pool of 500 unique data years (a  
 213 similar conceptual framework as suggested by (Fatichi et al., 2016)). For each  
 214 stochastic realization in the ensemble, the results consider only the average  
 215 conditions over the final three years of the 15-year simulation period. This

216 approach minimizes the impact of any one extreme year or set of climate  
217 conditions, while also highlighting the role of natural climate variations on  
218 the set of final results. Focusing on average conditions at the end of the  
219 simulation period is important because changes in salinity and sodicity levels  
220 sometimes take several years to manifest and stabilize.

221 In the results that follow, we focus on the following groups of scenarios,  
222 describing changes in evapotranspiration, rainfall season length, and extreme  
223 rainfall events intensity. All three groups share the same baseline scenario  
224 (Sec. 2.2), against which each treatment is compared.

225 **Evapotranspiration.** We describe nine scenarios, corresponding to  
226 additive changes between  $-0.5$  and  $+1.5$  mm d<sup>-1</sup> with respect to the  
227 baseline ET, with increments of 0.25 mm d<sup>-1</sup>. To minimize variation due to  
228 annual rainfall, these simulations use only the 50 colored trajectories in Fig.  
229 1a. The annual precipitation for each of these trajectories was within 10  
230 percent of the median annual total.

231 **Rainfall season length.** The baseline length of 190 days was multiplied  
232 by a factor between 0.6 to 1.2, with 0.1 increments, totaling seven scenarios.

233 **Extreme rainfall events** The highest 20% of rainfall events for each year  
234 were multiplied by a factor ranging from 0.5 to 2.0, with 0.25 increments.  
235 The smallest 20% of rainfall events were multiplied by the inverse of the  
236 factor. Within each group of scenarios, the simulations start using the same  
237 random seed, such that the hourly ET and rain inputs are identical across  
238 the groups, with the only differences due to the applied rainfall/ET factors.

239 In discussing the results, we introduce a modified aridity index. Because  
240 ET and precipitation can both vary across the simulation sets, the aridity

241 index is useful as a single metric for changes in water stress. Here, the  
242 aridity index is defined as the ratio of total evapotranspiration to the sum of  
243 all precipitation and irrigation inputs, i.e., higher values correspond to more  
244 arid conditions. The other input parameters used to run the simulations,  
245 including soil physical and chemical properties and the chemical composition  
246 of the irrigation water, are presented in Supplementary Materials 2.

### 247 **3. Results**

#### 248 *3.1. Effects of changing ET on soil system*

249 The simulations reveal a multi-faceted relationship between changing  
250 ET and the health of the soil system (Fig. 2). While salinity increases  
251 linearly with ET, the effects of ET on soil degradation are more varied,  
252 such that rising ET leads to higher unpredictability in relative  $K_s$ .  
253 Likewise, the relationship between relative  $K_s$  and salinity evolves as ET  
254 changes, eluding simple classification.

255 Fig. 2a shows the non-linear relationship between salinity and relative  
256 saturated hydraulic conductivity. As salinity increases, relative  $K_s$  values  
257 initially decline. When salinity levels exceed  $200 \text{ mmol}_c \text{ L}^{-1}$ , however, this  
258 trend reverses: relative  $K_s$  begins to increase and eventually surpass the  $K_s$   
259 values observed when salinity was lowest. We can also see that the  
260 relationship between salinity and relative  $K_s$  changes as aridity increases.  
261 Because variations in total rainfall in this set of simulations were limited,  
262 aridity index values are primarily a function of the input ET. We observe  
263 that the least desired results — high salinity and decreases in relative  $K_s$   
264 (at around  $200 \text{ mmol}_c \text{ L}^{-1}$ ) — occur as aridity increases. As aridity

265 increases, we also note that there is higher variability in the scatter of  
266 salinity and relative  $K_s$ ; the lowest aridity values (purple) are grouped  
267 closely together, while the high aridity (yellow) points are more spread out.

268 The sensitivity of salinity and sodicity to aridity is further explored in  
269 Fig. 2b-c. There is a significant linear relationship between increasing aridity  
270 and salinity in Fig. 2b ( $R^2$ : 0.95,  $p < 0.05$ ), with distinct clouds of points  
271 corresponding to the incremental jumps in input ET used in the simulations.  
272 Fig. 2c presents a significant negative, but less intense, trend in relative  $K_s$   
273 as aridity increases ( $R^2$ : 0.52,  $p < 0.05$ ), and emphasizes how relative  $K_s$  is  
274 prone to greater unpredictability as aridity increases.

### 275 *3.2. Effects of changing rainfall season length on soil system*

276 The simulation results show that longer rainfall seasons (lower aridity)  
277 lead to a noticeable decline in overall salinity and slight drops in relative  $K_s$   
278 (Fig. 3), and vice versa. These relationships are weak, however, in comparison  
279 to those observed when analyzing the effects of ET (note the scale differences  
280 between Fig. 2 and Fig. 3). Changes in rainfall season length lead to smaller  
281 ranges in aridity index, effectively leading to a less extreme set of climate  
282 conditions. Yet even within this limited range of aridity, the relationship  
283 between aridity and salinity and relative  $K_s$ , respectively, is less intense.  
284 Fig. 3b-c show that there is a wide scatter around the regression line for  
285 both salinity and relative  $K_s$ , indicating a wide range of potential salinity  
286 and relative  $K_s$  values for each aridity index value. This is further reflected in  
287 the relatively low  $R^2$  values for the relationship between salinity and aridity,  
288 and between relative  $K_s$  and aridity (0.39 and 0.12, respectively).

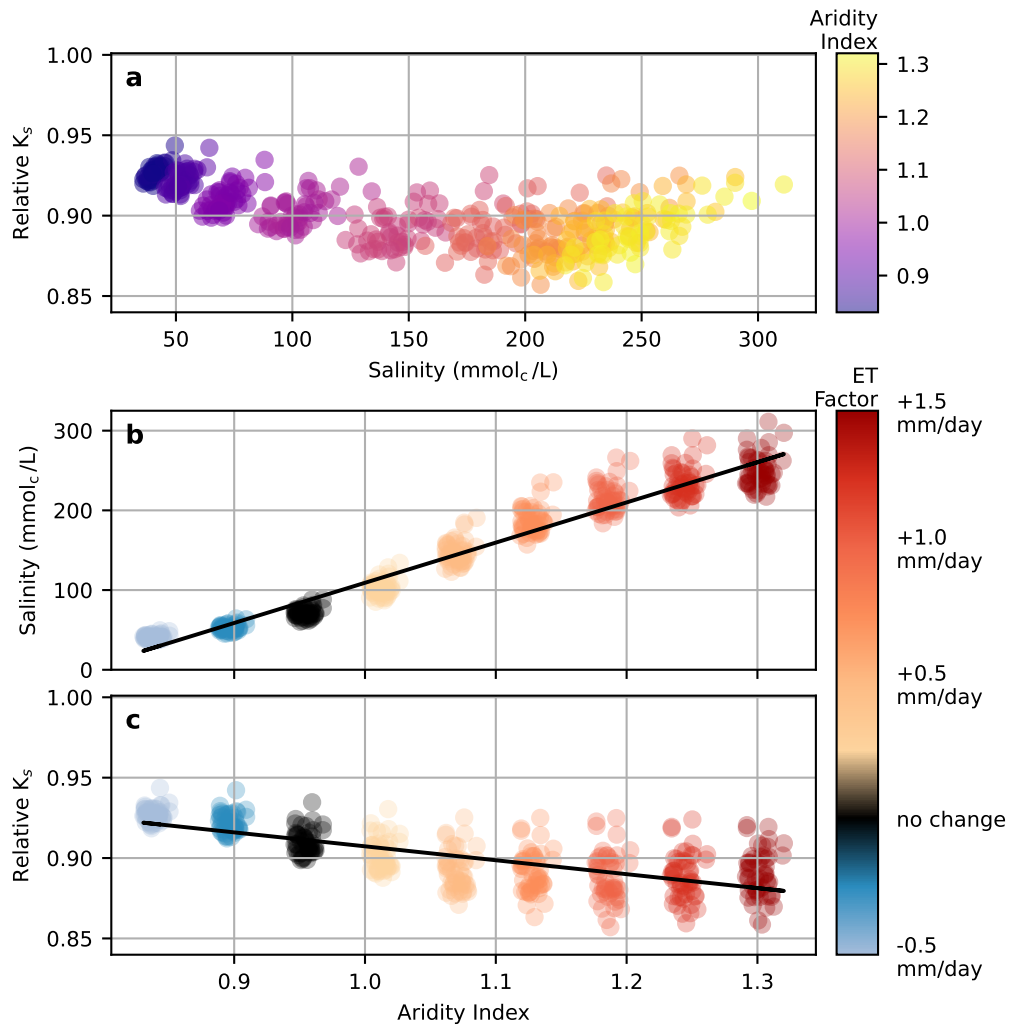


Figure 2: The effects of rising ET on the soil system. (a) The non-linear relationship between salinity and relative  $K_s$ . (b) the positive effect of rising ET on salinity ( $R^2$ : 0.95,  $p < 0.05$ ). (c) The negative relationship between ET and relative  $K_s$  ( $R^2$ : 0.52,  $p < 0.05$ ). Black lines are linear regression.

289 *3.3. Effects of extreme rainfall on soil system*

290 We found that an increase in the magnitude of the extreme rainfall events  
 291 leads to lower salinity and lower values of relative  $K_s$  (Fig. 4). The heavy



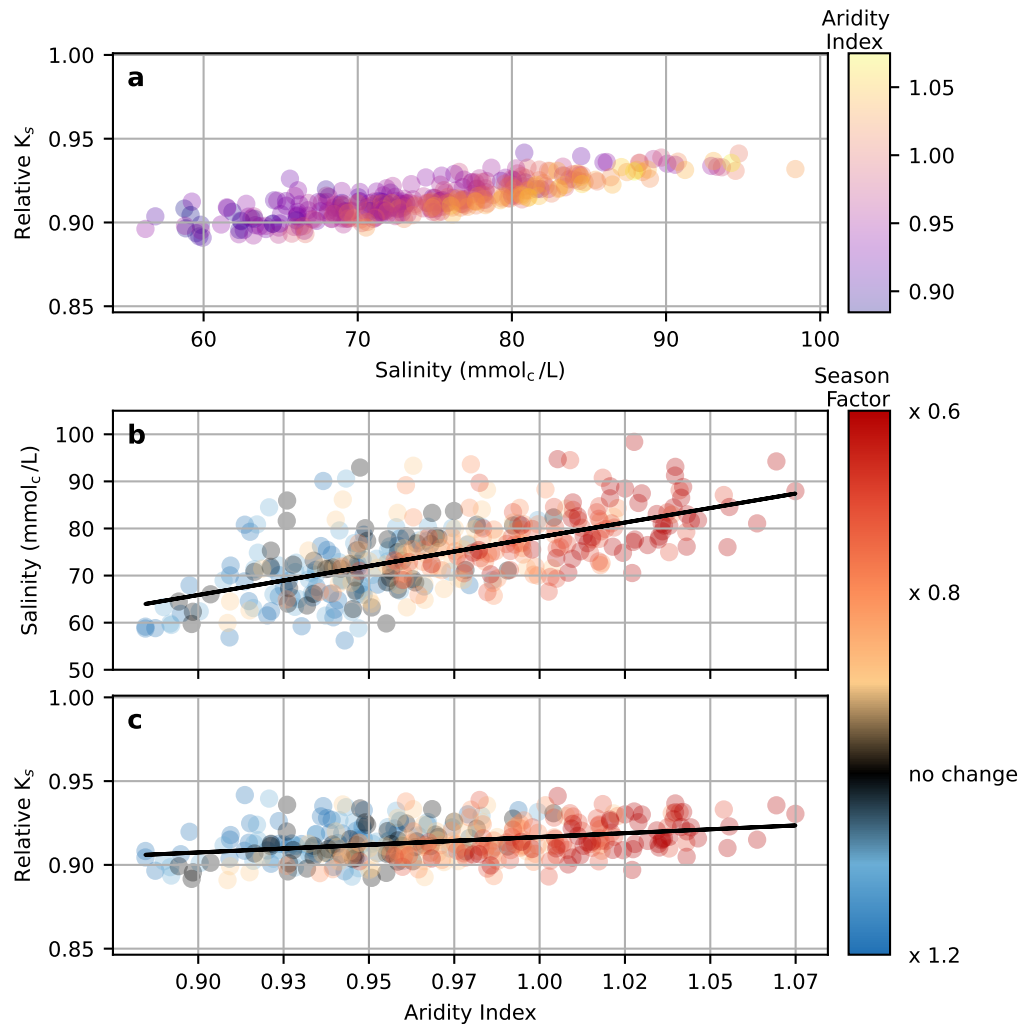


Figure 3: The effect of changes in rainfall season length on the soil system. (a) The relationship between salinity and relative  $K_s$ . (b) The effect of rainfall season length on salinity ( $R^2$ : 0.39). (c) The relationship between aridity and relative  $K_s$  ( $R^2$ : 0.12). Black lines are linear regression.

292 concentration of purple points in the bottom left of Fig. 4a corresponds to  
 293 the simulations with the lowest aridity values, which in this case are the

294 simulations with the highest magnitude of extreme rainfall events. Likewise,  
 295 Figs. 4b-c indicate positive linear relationships between aridity and salinity  
 296 and aridity and relative  $K_s$  ( $R^2$  values of 0.39 and 0.46, respectively).

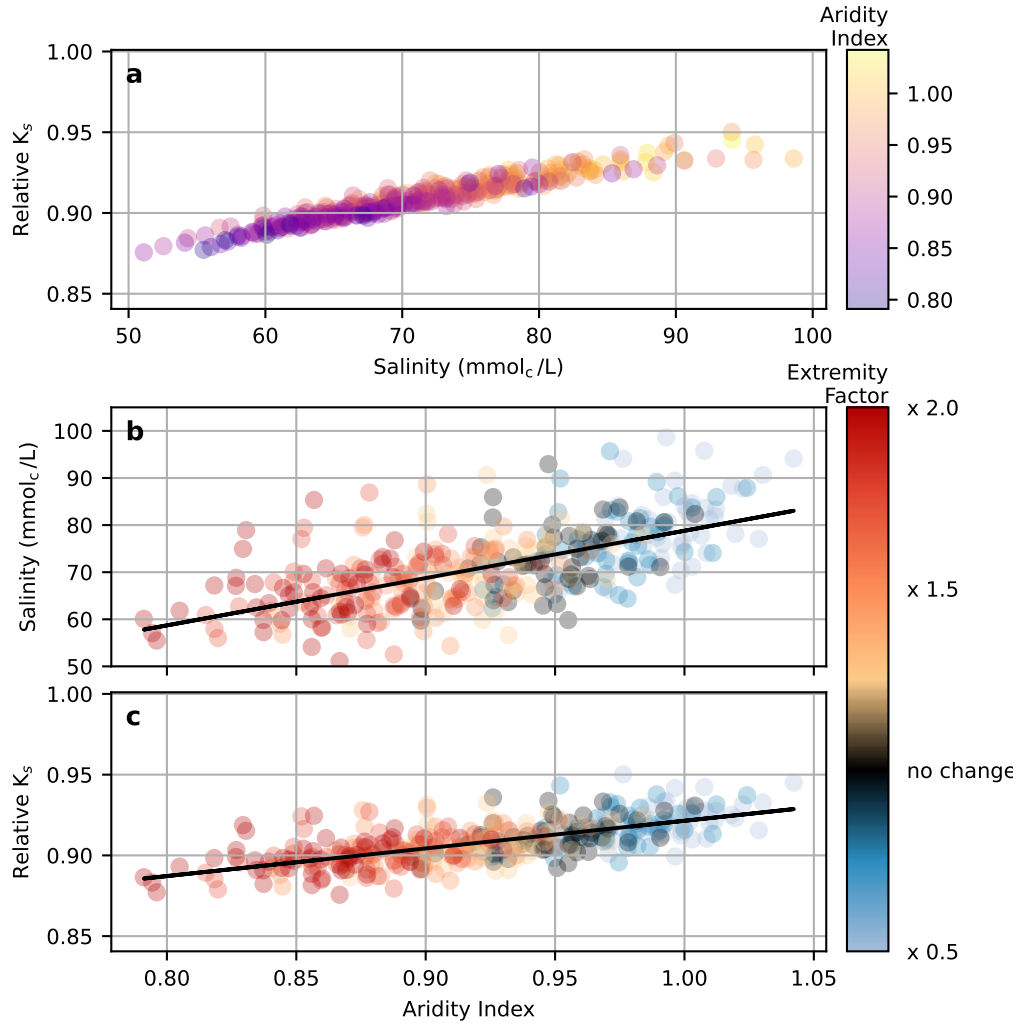


Figure 4: The effect of changes in extreme rainfall on soil system. (a) The relationship between salinity and relative  $K_s$ . (b) and (c) present the effect of extreme rainfall on salinity ( $R^2$ : 0.39) and relative  $K_s$  ( $R^2$ : 0.46), respectively. Black lines are linear regression.

## 297 4. Discussion

### 298 4.1. Shifting dynamics as a result of changes in $ET$

299 This shifting response of relative  $K_s$  dynamics observed in Sec. 3.1 is  
300 not entirely surprising given previous work on the effects of salinity and  
301 sodicity on  $K_s$ . Several experimental and modeling studies have  
302 demonstrated that seasonal fluctuations in salinity — typically as a result  
303 of high salinity irrigation water applied during dry months being leached by  
304 winter rainfall — have the potential to increase the risk of soil degradation  
305 (Shainberg and Shalhevet, 1984; van der Zee et al., 2014; Mau and  
306 Porporato, 2015; Kramer and Mau, 2020). This occurs because the fraction  
307 of sodium in the soil exchange complex changes at a slower rate than  
308 overall salinity, and degradation is most likely to occur when salinity is  
309 moderately low and the sodicity fraction relatively high (Shainberg and  
310 Shalhevet, 1984; van der Zee et al., 2014; Mau and Porporato, 2015;  
311 Kramer and Mau, 2020). These same studies, however, have demonstrated  
312 that extremely high levels of salinity are likely to insulate the soil system  
313 against degradation hazards, no matter how high the sodicity fraction. In  
314 these cases, extreme salinity levels mask the relatively weak ionic bonding  
315 strength of the sodium cations.

316 The similar distribution of the points within each of the clouds in the  $ET$   
317 simulations is a feature of the modeling setup. The same random seed was  
318 used before each simulation set to restrict variation in the final results to the  
319 effect of initial  $ET$  (Sec. 2.3). While differences in annual rainfall in this set  
320 of simulations were intentionally restricted, most of the variation in results  
321 at the selected  $ET$  increments can be explained by rainfall (Supplemental

322 Materials 3).

#### 323 *4.2. Rainfall vs. ET simulations*

324 The results from the rainfall season length (Sec. 3.2) and extreme  
325 rainfall (Sec. 3.3) exhibit several differences in comparison to the ET  
326 simulations (Sec. 3.1). In the ET simulations the relationship between  
327 salinity and relative  $K_s$  switches from a negative correlation to positive as  
328 salinity increases. The rainfall simulations, by contrast, feature a  
329 consistently negative relationship between the two variables. This is partly  
330 explained by the fact that the rainfall and ET simulations showcase a  
331 difference in the relationship between aridity and relative  $K_s$ . In the ET  
332 simulations, aridity and relative  $K_s$  have a moderately negative correlation,  
333 while in the rainfall simulations, the correlation between the two variables  
334 is slightly positive.

335 These differences point to important distinctions in how the selected  
336 climate variables affect the soil system. The ET simulations experience a  
337 wider range of salinity levels than observed in the rainfall simulations (the  
338 reader's attention is drawn to the different axis limits in Figs. 2–4).  
339 Specifically, the results show that for the scenarios examined, increasing ET  
340 drives higher salinity levels than in any of the rainfall simulations. It is also  
341 worth making clear that the extreme salinity levels recorded in the ET  
342 simulations are beyond the tolerance levels of even the most salt-resistant  
343 crops.

344 The model results suggest that farmers under such conditions would have  
345 no choice but to (a) spend more water by increasing the leaching fraction to  
346 stimulate the leaching of salts from the root zone, (b) search for irrigation

347 water with a less saline chemical composition or, (c) abandon agricultural  
348 production altogether. Given that such regions are already facing water  
349 scarcity, solutions (a) and (b) will be difficult to apply, while option (c)  
350 would endanger food security and economic output.

351 At the same aridity index values, the rainfall simulations exhibit lower  
352 salinity levels compared to the ET simulation. For example, when the  
353 aridity index value is 1, the ET simulations show an average salinity of  
354 approximately  $100 \text{ mmol}_c \text{ L}^{-1}$  (Fig. 2b), while the average salinity levels are  
355 less than  $80 \text{ mmol}_c \text{ L}^{-1}$  in the two rainfall simulations when the aridity  
356 index is 1 (Figs. 3b and 4b). One possible explanation for this difference is  
357 that the increased rainfall drives additional leaching of salts from the root  
358 zone. While leaching can certainly contribute to lower salinity values,  
359 Sec. 4.4 discusses some potential limitations concerning the model's ability  
360 to fully forecast the effects of extreme rainfall.

### 361 *4.3. Impact on soil health hazards*

362 One of the clearest contrasts between the three sets of simulations is  
363 how the changing climatic variables affect the overall hazard of dangerous  
364 salinity and relative  $K_s$  levels. This point is emphasized in Fig. 5, which  
365 presents probability density functions (PDFs) for each of the sets of  
366 scenarios. The PDFs for the ET simulations show the highest levels of  
367 variation, with rising ET strongly contributing to increased salinity hazards  
368 and soil degradation, affecting soil health and agriculture production. In  
369 Fig. 5a, the PDFs shift from right to left as ET increases, indicating lower  
370 averages for relative  $K_s$ , while in Fig. 5b the PDFs shift from left to right  
371 as ET increases, corresponding to elevated salinity levels. In both cases, not

372 only do the PDFs shift to the less desirable range of values, but the PDFs  
373 themselves become flatter, indicating a wider range of potential values –  
374 i.e., that the final results are characterized by higher levels of uncertainty.

375 These dynamics are present to a less significant degree in the other sets  
376 of simulations. As rainfall season length becomes shorter, the PDFs move  
377 rightward (Fig. 5c-d), consistent with the higher salinity values observed in  
378 Sec. 3.2. The PDFs also become narrower, indicating not only that the model  
379 forecasts increased salinity as ET rises, but also a high level of certainty in this  
380 outcome. The effect of rainfall season length on relative  $K_s$  has minimal effect  
381 on the PDFs, again consistent with the lower correlation observed between  
382 aridity and relative  $K_s$  in Fig. 3c. The PDFs for the rainfall extremity  
383 simulations exhibit a gradual shift to the left for the relative  $K_s$  output  
384 (Fig. 5e-f), while increased rainfall extremity actually causes the salinity  
385 PDFs to shift to the left.

#### 386 *4.4. Modeling limitations*

387 The simulations presented here help understand how salinity and  
388 sodicity dynamics might be affected by changes in climate, but inherent  
389 modeling limitations should be considered when assessing the results. The  
390 simulations were intentionally narrow in scope, focusing on sensitivity to a  
391 single climate feature at a time. While this approach is important for  
392 building initial understandings, it is more likely that future climate  
393 conditions will involve parallel changes to rainfall duration and intensity,  
394 ET, and possibly other variables. Future research should explore how  
395 interactions between climate variables will affect the system as a whole.  
396 While such an investigation is within the capabilities of the combined

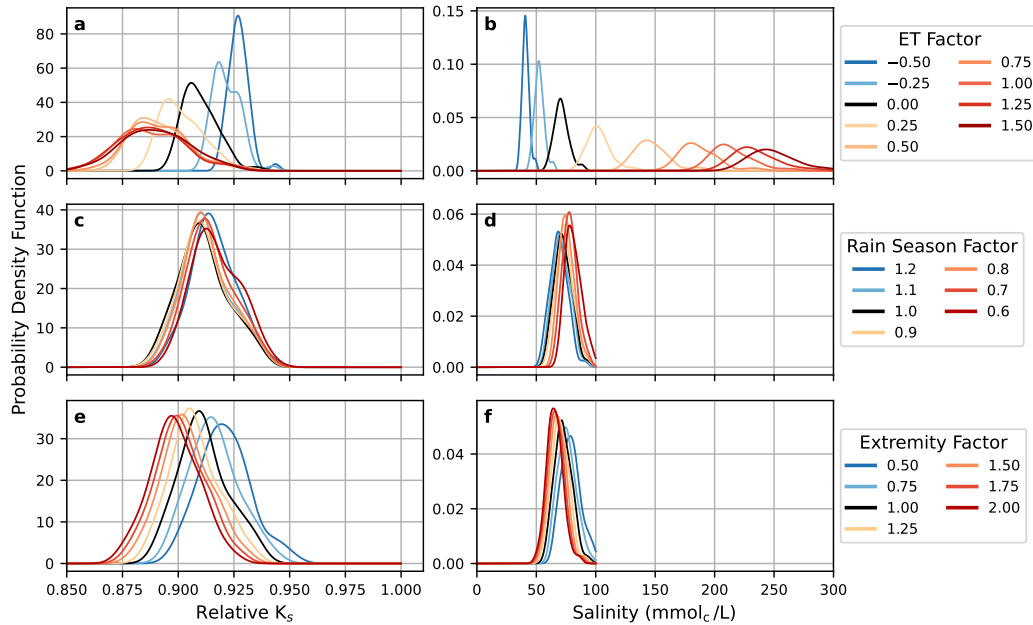


Figure 5: The probability distribution functions (PDFs) for relative  $K_s$  results for (a) ET, (c) rainfall season length, and (e) rainfall extremity simulations. (b), (d), and (f) present the PDFs for salinity values for the same sets of simulations.

397 SOTE-AWE-GEN framework, it is beyond the scope of this study.

398 Likewise, the present analysis focuses on changes to the soil root zone with  
 399 little attention to the interaction between different layers of the soil profile  
 400 or the potential effect of rainfall itself on a soil's physical conditions. While  
 401 SOTE is not by definition restricted to the analysis of specific soil depths,  
 402 it is a bucket model and therefore less amenable to studying interactions  
 403 between the upper and lower layers of the soil profile. We focused on the  
 404 upper layers of the soil profile since changes in salinity and infiltration rates  
 405 in the zone present an immediate risk to crop production. Attention to  
 406 lower layers of the profile, however, could be especially important in cases

407 where groundwater infiltration is of concern. Furthermore, the simulations  
408 in Sec. 3.3 focused on extreme rainfall events without analyzing the potential  
409 effects of impact force itself on the soil. It is well understood that extreme  
410 rainfall can lead to dispersion of the particles on the soil surface, including  
411 the breakdown of soil aggregates, such that infiltration rates and overall  
412 hydraulic conductivity are both impacted (Assouline, 2004). To increase  
413 our understanding of how extreme rainfall might affect salinity and sodicity  
414 dynamics, the incorporation of these phenomena should be considered an  
415 important next step.

## 416 5. Conclusion

417 We analyzed the first-order sensitivity of salinity and sodicity dynamics  
418 to changes in ET, rainfall season length, and extreme rainfall. While  
419 increased aridity leads to higher salinity levels in all three sets of  
420 simulations, the response of relative  $K_s$  showed mixed behavior – with  
421 increased aridity leading to lower relative  $K_s$  in the ET simulations, and  
422 slightly higher relative  $K_s$  in the rainfall simulations. Changes in  
423 temperature (ET) led to the largest variation in output levels, with higher  
424 ET contributing to wider distribution in final salinity and relative  $K_s$ .

425 Climate models have consistently pointed to a likely rise in temperature  
426 and ET in the Fresno area, underscoring the importance of understanding  
427 how these changes may affect soil health. The exact nature of any future  
428 climate will of course depend on government policy, technological  
429 developments, and potential feedback between climate variables. However,  
430 a substantial rise in temperature and ET, on the order of that explored in



431 this research, is well within the range of possible changes, presenting a  
432 potentially serious threat to agricultural production.

433 The analyses here used the San Joaquin Valley as a case study, but the  
434 results are a bellwether for other agriculturally important parts of the US  
435 and beyond. Farmers throughout the rest of California, the American  
436 Southwest, and large portions of the Midwest are similarly confronted by  
437 the challenges of declining freshwater access and expected temperature  
438 increases, while simultaneously facing pressure to improve crop yields as  
439 food demand grows. Furthermore, the general climate patterns in Fresno  
440 County – hot and dry summer growing seasons; seasonal rainfall during the  
441 winter months – are common in other regions affected by salinity and  
442 sodicity hazards, including large portions of the Middle East and North  
443 Africa, the Indian sub-continent, and Australia (Kramer and Mau, 2023;  
444 FAO, 2023).

445 What most separates the San Joaquin Valley from these other regions is  
446 the California agricultural sector’s relatively strong ability to cope with  
447 climate-driven challenges. Traditionally, the most effective ways of  
448 mitigating salinity hazards are irrigation with higher quality (low-salinity)  
449 input water, intentional over-irrigation designed to leach salts from the root  
450 zone, and transition to more salt-tolerant crops and varieties. Many  
451 growers in the San Joaquin Valley focus on high-revenue specialty crops,  
452 providing them with the capital necessary to invest in high-efficiency  
453 irrigation systems, advanced monitoring capabilities, and automation  
454 equipment – all of which can contribute to water conservation. Likewise,  
455 these growers are more capable of transitioning to salt-resistant varieties.

456 Several local, state, and national funding programs provide further financial  
457 aid and direct incentives to farmers interested in technological upgrades.  
458 Abundant government funding can help support investment in alternatives  
459 such as desalination and treated wastewater, which can provide  
460 supplemental sources of irrigation water when freshwater is limited. On the  
461 other hand, coping with the challenges of salinity and sodicity will be much  
462 more challenging in less wealthy regions, where investment in new  
463 technologies is less affordable for most food producers, and where  
464 governments are less capable of funding water infrastructure projects.

## 465 **References**

- 466 Adeyemo, T., Kramer, I., Levy, G.J., Mau, Y., 2022. Salinity and sodicity  
467 can cause hysteresis in soil hydraulic conductivity. *Geoderma* 413, 115765.  
468 doi:10.1016/j.geoderma.2022.115765.
- 469 Amundson, R.G., Lund, L.J., 1985. Changes in the chemical and  
470 physical properties of a reclaimed saline-sodic soil in the san  
471 joaquin valley of california. *Soil Science* 140, 213–222. URL:  
472 [https://journals.lww.com/soilsci/abstract/1985/09000/changes\\_](https://journals.lww.com/soilsci/abstract/1985/09000/changes_in_the_chemical_and_physical_properties_of.9.aspx)  
473 [in\\_the\\_chemical\\_and\\_physical\\_properties\\_of.9.aspx](https://journals.lww.com/soilsci/abstract/1985/09000/changes_in_the_chemical_and_physical_properties_of.9.aspx).
- 474 Amundson, R.G., Smith, V., 1988. Effects of irrigation on the chemical  
475 properties of a soil in the western san joaquin valley, california. *Arid Soil*  
476 *Research and Rehabilitation* 2, 1–17. doi:10.1080/15324988809381154.
- 477 Assouline, S., 2004. Rainfall-induced soil surface sealing: A critical review

478 of observations, conceptual models, and solutions. *Vadose Zone Journal* 3,  
479 570–591. doi:10.2136/vzj2004.0570.

480 Assouline, S., Narkis, K., 2011. Effects of long-term irrigation with treated  
481 wastewater on the hydraulic properties of a clayey soil. *Water Resources*  
482 *Research* 47, 1–12. doi:10.1029/2011WR010498.

483 Assouline, S., Russo, D., Silber, A., Or, D., 2015. Balancing water scarcity  
484 and quality for sustainable irrigated agriculture. *Water Resources Research*  
485 51, 3419–3436. doi:10.1002/2015WR017071.

486 Bardhan, G., Russo, D., Goldstein, D., Levy, G.J., 2016. Changes in the  
487 hydraulic properties of a clay soil under long-term irrigation with treated  
488 wastewater. *Geoderma* 264, 1–9. doi:10.1016/j.geoderma.2015.10.004.

489 Bernstein, L., 1975. Effects of salinity and sodicity on plant growth. *Annual*  
490 *Review of Phytopathology* 13, 295–312. doi:10.1146/annurev.py.13.  
491 090175.001455.

492 Bhardwaj, A.K., Mandal, U.K., Bar-Tal, A., Gilboa, A., Levy, G.J., 2008.  
493 Replacing saline-sodic irrigation water with treated wastewater: Effects on  
494 saturated hydraulic conductivity, slaking, and swelling. *Irrigation Science*  
495 26, 139–146. doi:10.1007/s00271-007-0080-1.

496 Bixio, D., Thoeye, C., Koning, J.D., Joksimovic, D., Savic, D., Wintgens, T.,  
497 Melin, T., 2006. Wastewater reuse in europe. *Desalination* 187, 89–101.  
498 doi:10.1016/j.desal.2005.04.070.

499 Cache, T., Ramirez, J.A., Molnar, P., Ruiz-Villanueva, V., Peleg, N., 2023.  
500 Increased erosion in a pre-alpine region contrasts with a future decrease in

501 precipitation and snowmelt. *Geomorphology* 436, 108782. doi:10.1016/  
502 j.geomorph.2023.108782.

503 Corwin, D.L., 2021. Climate change impacts on soil salinity in agricultural  
504 areas. *European Journal of Soil Science* 72, 842–862. doi:10.1111/ejss.  
505 13010.

506 Daliakopoulos, I., Tsanis, I., Koutroulis, A., Kourgialas, N., Varouchakis, A.,  
507 Karatzas, G., Ritsema, C., 2016. The threat of soil salinity: A european  
508 scale review. *Science of The Total Environment* 573, 727–739. doi:10.  
509 1016/j.scitotenv.2016.08.177.

510 Dinar, A., Aillery, M.P., Moore, M.R., 1993. A dynamic model of soil salinity  
511 and drainage generation in irrigated agriculture: A framework for policy  
512 analysis. *Water resources research* 29, 1527–1537. doi:10.1029/93WR00181.

513 Eaton, F.M., 1935. Boron in soils and irrigation waters and its effects on  
514 plants, with particular reference to the san joaquin valley of california.  
515 Technical Bulletin 448, 131. URL: [https://ageconsearch.umn.edu/  
516 record/164477/files/tb448.pdf](https://ageconsearch.umn.edu/record/164477/files/tb448.pdf). reference bibliography: 42.

517 FAO, 2023. Global salt-affected soils map (v2.0). URL: [https:  
518 //www.fao.org/soils-portal/data-hub/soil-maps-and-databases/  
519 global-map-of-salt-affected-soils/en/](https://www.fao.org/soils-portal/data-hub/soil-maps-and-databases/global-map-of-salt-affected-soils/en/).

520 FAO, ITPS, 2015. Status of the World’s Soil Resources. Food and Agriculture  
521 Organization of the United Nations and Intergovernmental Technical Panel  
522 on Soils. URL: [https://openknowledge.fao.org/server/api/core/  
523 bitstreams/6ec24d75-19bd-4f1f-b1c5-5becf50d0871/content](https://openknowledge.fao.org/server/api/core/bitstreams/6ec24d75-19bd-4f1f-b1c5-5becf50d0871/content).

- 524 Fatichi, S., Ivanov, V., Caporali, E., 2013. Assessment of a stochastic  
525 downscaling methodology in generating an ensemble of hourly future  
526 climate time series. *Climate Dynamics* 40, 1841–1861. doi:10.1007/  
527 s00382-012-1627-2.
- 528 Fatichi, S., Ivanov, V.Y., Caporali, E., 2011. Simulation of future climate  
529 scenarios with a weather generator. *Advances in Water Resources* 34, 448–  
530 467. doi:10.1016/j.advwatres.2010.12.013.
- 531 Fatichi, S., Ivanov, V.Y., Paschalis, A., Peleg, N., Molnar, P., Rimkus, S.,  
532 Kim, J., Burlando, P., Caporali, E., 2016. Uncertainty partition challenges  
533 the predictability of vital details of climate change. *Earth’s Future* 4, 240–  
534 251. doi:10.1002/2015EF000336.
- 535 Fatichi, S., Peleg, N., Mastrotheodoros, T., Pappas, C., Manoli, G., 2021.  
536 An ecohydrological journey of 4500 years reveals a stable but threatened  
537 precipitation–groundwater recharge relation around jerusalem. *Science*  
538 *Advances* 7, eabe6303. doi:10.1126/sciadv.abe6303.
- 539 Fernández, E., 2023. Editorial note on terms for crop evapotranspiration,  
540 water use efficiency and water productivity. *Agricultural Water*  
541 *Management* 289, 108548. doi:10.1016/j.agwat.2023.108548.
- 542 Fowler, H.J., Lenderink, G., Prein, A.F., Westra, S., Allan, R.P., Ban, N.,  
543 Barbero, R., Berg, P., Blenkinsop, S., Do, H.X., et al., 2021. Anthropogenic  
544 intensification of short-duration rainfall extremes. *Nature Reviews Earth*  
545 *& Environment* 2, 107–122. doi:10.1038/s43017-020-00128-6.

- 546 Fujii, R., Deverel, S., Hatfield, D., 1988. Distribution of selenium in soils  
547 of agricultural fields, western san joaquin valley, california. Soil Science  
548 Society of America Journal 52, 1274–1283. doi:10.2136/sssaj1988.  
549 03615995005200050011x.
- 550 Gonçalves, M.C., Šimůnek, J., Ramos, T.B., Martins, J.C., Neves, M.J.,  
551 Pires, F.P., 2006. Multicomponent solute transport in soil lysimeters  
552 irrigated with waters of different quality. Water Resources Research 42,  
553 1–17. doi:10.1029/2005WR004802.
- 554 Hansen, J.A., Jurgens, B.C., Fram, M.S., 2018. Quantifying anthropogenic  
555 contributions to century-scale groundwater salinity changes, San Joaquin  
556 Valley, California, USA. Science of the Total Environment 642, 125–136.  
557 doi:10.1016/j.scitotenv.2018.05.333.
- 558 Hanson, B., May, D., 2003. Drip irrigation increases tomato yields in salt-  
559 affected soil of san joaquin valley. California Agriculture 57. URL: <https://escholarship.org/uc/item/2kj1899w>.
- 561 Hassani, A., Azapagic, A., Shokri, N., 2020. Predicting long-term dynamics  
562 of soil salinity and sodicity on a global scale. Proceedings of the National  
563 Academy of Sciences 117, 33017–33027. doi:10.1073/pnas.2013771117.
- 564 Hassani, A., Azapagic, A., Shokri, N., 2021. Global predictions of primary  
565 soil salinization under changing climate in the 21st century. Nature  
566 Communications 12, 1–17. doi:10.1038/s41467-021-26907-3.
- 567 Howitt, R.E., Kaplan, J., Larson, D., MacEwan, D., Medellín-  
568 Azuara, J., Horner, G., Lee, N.S., 2009. The economic impacts

569 of Central Valley salinity. Final Report to the State Water  
570 Resources Control Board Contract. University of California  
571 Davis. URL: [https://www.remi.com/topics-and-studies/  
572 the-economic-impacts-of-central-valley-salinity/](https://www.remi.com/topics-and-studies/the-economic-impacts-of-central-valley-salinity/).

573 Ivanov, V.Y., Bras, R.L., Curtis, D.C., 2007. A weather generator for  
574 hydrological, ecological, and agricultural applications. Water Resources  
575 Research 43. doi:10.1029/2006WR005364.

576 Knapp, K.C., 1992a. Irrigation management and investment under saline,  
577 limited drainage conditions: 1. model formulation. Water Resources  
578 Research 28, 3085–3090. doi:10.1029/92WR01747.

579 Knapp, K.C., 1992b. Irrigation management and investment under saline,  
580 limited drainage conditions: 2. characterization of optimal decision rules.  
581 Water Resources Research 28, 3091–3097. doi:10.1029/92WR01746.

582 Knapp, K.C., 1992c. Irrigation management and investment under saline,  
583 limited drainage conditions: 3. policy analysis and extensions. Water  
584 resources research 28, 3099–3109. doi:10.1029/92WR01745.

585 Kramer, I., Bayer, Y., Adeyemo, T., Mau, Y., 2021. Hysteresis in  
586 soil hydraulic conductivity as driven by salinity and sodicity – a  
587 modeling framework. Hydrology and Earth System Sciences 25, 1993–  
588 2008. URL: <https://hess.copernicus.org/articles/25/1993/2021/>,  
589 doi:10.5194/hess-25-1993-2021.

590 Kramer, I., Bayer, Y., Mau, Y., 2022a. The Sustainability of Treated  
591 Wastewater Irrigation: The Impact of Hysteresis on Saturated Soil

592 Hydraulic Conductivity. *Water Resources Research* 58, 1–14. doi:10.1029/  
593 2021wr031307.

594 Kramer, I., Mau, Y., 2020. Soil Degradation Risks Assessed by the SOTE  
595 Model for Salinity and Sodicity. *Water Resources Research* 56. doi:10.  
596 1029/2020WR027456.

597 Kramer, I., Mau, Y., 2023. Review: Modeling the effects of salinity  
598 and sodicity in agricultural systems. *Water Resources Research* 59,  
599 e2023WR034750. doi:10.1029/2023WR034750.

600 Kramer, I., Tsairi, Y., Roth, M.B., Tal, A., Mau, Y., 2022b. Effects of  
601 population growth on israel’s demand for desalinated water. *npj Clean*  
602 *Water* 5, 67. doi:10.1038/s41545-022-00215-9.

603 Kroes, J., van Dam, J., Bartholomeus, R., Groenendijk, P., Heinen,  
604 M., Hendriks, R., Mulder, H., Supit, I., van Walsum, P., 2017.  
605 SWAP version 4. Wageningen Environmental Research. Wageningen,  
606 The Netherlands. URL: [https://research.wur.nl/en/publications/  
607 swap-version-4](https://research.wur.nl/en/publications/swap-version-4). software description and user manual.

608 Lado, M., Bar-Tal, A., Azenkot, A., Assouline, S., Ravina, I., Erner,  
609 Y., Fine, P., Dasberg, S., Ben-Hur, M., 2012. Changes in chemical  
610 properties of semiarid soils under long-term secondary treated  
611 wastewater irrigation. *Soil Science Society of America Journal* 76,  
612 1358–1369. URL: [https://access.onlinelibrary.wiley.com/  
613 doi/abs/10.2136/sssaj2011.0230](https://access.onlinelibrary.wiley.com/doi/abs/10.2136/sssaj2011.0230), doi:10.2136/sssaj2011.0230,  
614 arXiv:<https://access.onlinelibrary.wiley.com/doi/pdf/10.2136/sssaj2011.0230>.



- 615 Levy, G.J., 2011. Impact of long-term irrigation with treated wastewater  
616 on soil-structure stability— the israeli experience. *Israel Journal of Plant*  
617 *Sciences* 59, 95–104. doi:10.1560/IJPS.59.2-4.95.
- 618 Lin, Z.Q., Schemenauer, R.S., Cervinka, V., Zayed, A., Lee, A., Terry,  
619 N., 2000. Selenium volatilization from a soil—plant system for the  
620 remediation of contaminated water and soil in the san joaquin valley.  
621 *Journal of Environmental Quality* 29, 1048–1056. doi:10.2134/jeq2000.  
622 00472425002900040003x.
- 623 Ma, L., Ahuja, L., Nolan, B.T., Malone, R., Trout, T., Qi, Z.,  
624 2012. Root zone water quality model (rzwqm2): Model use,  
625 calibration and validation. *Transactions of the ASABE* 55, 1425–1446.  
626 URL: [https://www.ars.usda.gov/ARSEUserFiles/3495/26.%20SW9454%](https://www.ars.usda.gov/ARSEUserFiles/3495/26.%20SW9454%20with%20corrected%20p%201445.pdf)  
627 [20with%20corrected%20p%201445.pdf](https://www.ars.usda.gov/ARSEUserFiles/3495/26.%20SW9454%20with%20corrected%20p%201445.pdf).
- 628 Maas, E.V., Grattan, S.R., 1999. Crop yields as affected by salinity,  
629 in: *Agricultural Drainage*. John Wiley & Sons, Ltd, pp. 55–  
630 108. URL: <http://doi.wiley.com/10.2134/agronmonogr38.c3>, doi:10.  
631 2134/agronmonogr38.c3.
- 632 Mandal, U.K., Bhardwaj, A.K., Warrington, D.N., Goldstein, D., Bar-Tal,  
633 A., Levy, G.J., 2008. Changes in soil hydraulic conductivity, runoff, and soil  
634 loss due to irrigation with different types of saline-sodic water. *Geoderma*  
635 144, 509–516. doi:10.1016/j.geoderma.2008.01.005.
- 636 Marra, F., Koukoula, M., Canale, A., Peleg, N., 2024. Predicting  
637 extreme sub-hourly precipitation intensification based on temperature

638 shifts. *Hydrology and Earth System Sciences* 28, 375–389. doi:10.5194/  
639 hess-28-375-2024.

640 Mau, Y., Porporato, A., 2015. A dynamical system approach to soil salinity  
641 and sodicity. *Advances in Water Resources* 83, 68–76. doi:10.1016/j.  
642 advwatres.2015.05.010.

643 McGeorge, W.T., 1954. Diagnosis and improvement of saline and alkaline  
644 soils. *Soil Science Society of America Journal* 18, 348. doi:10.2136/  
645 sssaj1954.03615995001800030032x.

646 Minhas, P.S., Ramos, T.B., Ben-Gal, A., Pereira, L.S., 2020. Coping  
647 with salinity in irrigated agriculture: Crop evapotranspiration and water  
648 management issues. *Agricultural Water Management* 227. doi:10.1016/  
649 j.agwat.2019.105832.

650 Mitchell, J.P., Shrestha, A., Mathesius, K., Scow, K.M., Southard, R.J.,  
651 Haney, R.L., Schmidt, R., Munk, D.S., Horwath, W.R., 2017. Cover  
652 cropping and no-tillage improve soil health in an arid irrigated cropping  
653 system in california’s san joaquin valley, usa. *Soil and Tillage Research*  
654 165, 325–335. doi:10.1016/j.still.2016.09.001.

655 Munns, R., 2002. Comparative physiology of salt and water stress. *Plant, Cell  
656 & Environment* 25, 239–250. doi:10.1046/j.0016-8025.2001.00808.x.

657 Nelson, J.W., Guernsey, J.E., Holmes, L.C., Eckmann, E.C., 1918.  
658 Reconnaissance Soil Survey of the Lower San Joaquin Valley, California.  
659 U.S. Department of Agriculture, Soil Conservation Service, Washington,  
660 D.C. No specific publication date available.

- 661 Oster, J.D., 1994. Irrigation with poor quality water. *Agricultural Water*  
662 *Management* 25, 271–297. doi:10.1016/0378-3774(94)90064-7.
- 663 Peel, M.C., Finlayson, B.L., McMahon, T.A., 2007. Updated world map of  
664 the Köppen-geiger climate classification. *Hydrology and Earth System*  
665 *Sciences* 11, 1633–1644. doi:10.5194/hess-11-1633-2007.
- 666 Peleg, N., Skinner, C., Fatichi, S., Molnar, P., 2020. Temperature  
667 effects on the spatial structure of heavy rainfall modify catchment hydro-  
668 morphological response. *Earth Surface Dynamics* 8, 17–36. doi:10.5194/  
669 *esurf*-8-17-2020.
- 670 Pierce, D.W., Das, T., Cayan, D.R., Maurer, E.P., Miller, N.L.,  
671 Bao, Y., Kanamitsu, M., Yoshimura, K., Snyder, M.A., Sloan, L.C.,  
672 Franco, G., Tyree, M., 2013. Probabilistic estimates of future  
673 changes in California temperature and precipitation using statistical and  
674 dynamical downscaling. *Climate Dynamics* 40, 839–856. doi:10.1007/  
675 *s00382-012-1337-9*.
- 676 Prăvălie, R., Patriche, C., Borrelli, P., Panagos, P., Roșca, B., Dumitrașcu,  
677 M., Nita, I.A., Săvulescu, I., Birsan, M.V., Bandoc, G., 2021. Arable  
678 lands under the pressure of multiple land degradation processes. a global  
679 perspective. *Environmental Research* 194. doi:10.1016/j.*envres*.2020.  
680 110697.
- 681 Qadir, M., Quillérrou, E., Nangia, V., Murtaza, G., Singh, M., Thomas,  
682 R.J., Drechsel, P., Noble, A.D., 2014. Economics of salt-induced land

683 degradation and restoration. *Natural Resources Forum* 38, 282–295.  
684 doi:10.1111/1477-8947.12054.

685 Quinn, N.W.T., 2020. Policy Innovation and Governance for Irrigation  
686 Sustainability in the Arid, Saline San Joaquin River Basin. *Sustainability*  
687 12, 4733. doi:10.3390/su12114733.

688 Ramirez, J.A., Peleg, N., Baird, A.J., Young, D.M., Morris, P.J., Larocque,  
689 M., Garneau, M., 2023. Modelling peatland development in high-boreal  
690 quebec, canada, with digibog\_boreal. *Ecological Modelling* 478, 110298.  
691 doi:10.1016/j.ecolmodel.2023.110298.

692 Razavi, S., Gupta, H.V., 2015. What do we mean by sensitivity analysis? the  
693 need for comprehensive characterization of “global” sensitivity in earth and  
694 environmental systems models. *Water Resources Research* 51, 3070–3092.  
695 URL: 10.1002/2014WR016527.

696 Russo, D., 1984. A geostatistical approach to solute transport in  
697 heterogeneous fields and its applications to salinity management. *Water*  
698 *Resources Research* 20, 1260–1270. doi:10.1029/WR020i009p01260.

699 Russo, D., 1988. Numerical analysis of the nonsteady transport of interacting  
700 solutes through unsaturated soil: 1. homogeneous systems. *Water*  
701 *Resources Research* 24, 271–284. doi:10.1029/WR024i002p00271.

702 Russo, D., 2013. Consequences of salinity-induced-time-dependent soil  
703 hydraulic properties on flow and transport in salt-affected soils. *Procedia*  
704 *Environmental Sciences* 19, 623–632. doi:10.1016/j.proenv.2013.06.  
705 071.

- 706 Russo, D., Zaidel, J., Laufer, A., 2004. Numerical analysis of transport of  
707 interacting solutes in a three-dimensional unsaturated heterogeneous soil.  
708 *Vadose Zone Journal* 3, 1286–1299. doi:10.2136/vzj2004.1286.
- 709 Schacht, K., Marschner, B., 2015. Treated wastewater irrigation effects  
710 on soil hydraulic conductivity and aggregate stability of loamy soils in  
711 israel. *Journal of Hydrology and Hydromechanics* 63, 47–54. doi:10.1515/  
712 johh-2015-0010.
- 713 Schoups, G., Hopmans, J.W., Young, C.A., Panday, S., 2005. Sustainability  
714 of irrigated agriculture in the san joaquin valley, california. *Proceedings of*  
715 *the National Academy of Sciences* 102, 15352–15356. doi:10.1073/pnas.  
716 0507723102.
- 717 Scudiero, E., Skaggs, T.H., Corwin, D.L., 2014. Regional scale soil salinity  
718 evaluation using landsat 7, western san joaquin valley, california, usa.  
719 *Geoderma Regional* 2-3, 82–90. doi:10.1016/j.geodrs.2014.10.004.
- 720 Shah, S.H., Vervoort, R.W., Suweis, S., Guswa, A.J., Rinaldo, A., Zee,  
721 S.E.V.D., 2011. Stochastic modeling of salt accumulation in the root zone  
722 due to capillary flux from brackish groundwater. *Water Resources Research*  
723 47, 1–17. doi:10.1029/2010WR009790.
- 724 Shainberg, I., Shalhevet, J. (Eds.), 1984. *Soil Salinity Under*  
725 *Irrigation: Processes and Management*. Springer-Verlag. doi:10.1007/  
726 978-3-642-69836-1.
- 727 Tanji, K.K., Doneen, L.D., Ferry, G.V., Ayers, R.S., 1972. Computer  
728 simulation analysis on reclamation of salt-affected soils in san joaquin

- 729 valley, california. Soil Science Society of America Journal 36, 127–133.  
730 doi:10.2136/sssaj1972.03615995003600010030x.
- 731 Thellier, C., Holtzclaw, K.M., Rhoades, J.D., Sposito, G., 1990. Chemical  
732 effects of saline irrigation water on a san joaquin valley soil: Ii. field  
733 soil samples. Journal of Environmental Quality 19, 56–60. doi:10.2134/  
734 jeq1990.00472425001900010006x.
- 735 Tidball, R.R., Severson, R.C., Gent, C.A., Riddle, G.O., 1989. Element  
736 Associations in Soils of the San Joaquin Valley of California. John Wiley  
737 & Sons, Ltd. chapter 9. pp. 179–193. doi:10.2136/sssaspecpub23.c9.
- 738 Wallender, W.W., Tanji, K.K. (Eds.), 2011. Agricultural Salinity Assessment  
739 and Management. 2nd ed. ed., American Society of Civil Engineers.  
740 doi:10.1061/9780784411698.
- 741 Yin, X., Feng, Q., Li, Y., Liu, W., Zhu, M., Xu, G., Zheng, X., Sindikubwabo,  
742 C., 2021. Induced soil degradation risks and plant responses by salinity  
743 and sodicity in intensive irrigated agro-ecosystems of seasonally-frozen arid  
744 regions. Journal of Hydrology 603, 127036. doi:10.1016/j.jhydro1.2021.  
745 127036.
- 746 Yin, X., Feng, Q., Liu, W., Zhu, M., Zhang, J., Li, Y., Yang, L., Zhang,  
747 C., Cui, M., Zheng, X., Li, Y., 2023. Assessment and mechanism analysis  
748 of plant salt tolerance regulates soil moisture dynamics and controls root  
749 zone salinity and sodicity in seasonally irrigated agroecosystems. Journal  
750 of Hydrology 617, 129138. doi:10.1016/j.jhydro1.2023.129138.

- 751 van der Zee, S., Shah, S., Vervoort, R., 2014. Root zone salinity and  
752 sodicity under seasonal rainfall due to feedback of decreasing hydraulic  
753 conductivity. *Water Resources Research* 50, 9432–9446. doi:10.1002/  
754 2013WR015208.
- 755 van der Zee, S., Shah, S.H., van Uffelen, C.G., Raats, P.A., dal Ferro, N.,  
756 2010. Soil sodicity as a result of periodical drought. *Agricultural Water*  
757 *Management* 97, 41–49. doi:10.1016/j.agwat.2009.08.009.
- 758 Šimůnek, J., Sakai, M., Genuchten, M.V., Saito, H., Sejna, M., 2013.  
759 The HYDRUS-1D Software Package for Simulating the One-Dimensional  
760 Movement of Water, Heat, and Multiple Solutes in Variably-Saturated  
761 Media. Department of Environmental Sciences, University of California  
762 Riverside. Riverside, California. URL: [https://www.pc-progress.com/  
763 Downloads/Pgm\\_hydrus1D/HYDRUS1D-4.08.pdf](https://www.pc-progress.com/Downloads/Pgm_hydrus1D/HYDRUS1D-4.08.pdf). version 4.17.
- 764 Šimůnek, J., Suarez, D.L., 1994. Two-dimensional transport model for  
765 variably saturated porous media with major ion chemistry. *Water*  
766 *Resources Research* 30, 1115–1133. doi:10.1029/93WR03347.